Available online at www.sciencedirect.com
ScienceDirect
Procedia CIRP 13 (2014) 417 – 422

www.elsevier.com/locate/procedia

2nd CIRP 2nd CIRP Conference on Surface Integrity (CSI)

Surface Quality Analysis of Titanium and Nickel-based Alloys Using Picosecond Laser

Ming Chu Kong*, Jie Wang

University of Liverpool, Liverpool, B15 2TT, United Kingdom
* Corresponding author. C.Kong@bham.ac.uk

Abstract

In order to evaluate the surface quality of ablated Ti-6Al-4V and Ni-Ti with a widely used 10-picosecond laser system with a wavelength of 1064 NM at a repetition rate of 5 kHz, three stages have been accomplished: i) study of the material removal mechanism on single cracters; ii) investigation of process parameters on surface finishing of linear tracks; iii) evaluation of the (sub-) surface of laser-ablated pockets. Through studying the influence of laser fluencies on single cracters, the evolution of component surface involved in the laser ablation has been obtained. This is further supported by investigating the threshold fluence, incubation effect and surface morphology of the ablated cracters. Ti-6Al-4V is found to have a higher incubation that indicates its weaker accumulation ability of heat of plastic deformation. Cavity-like structures are observed in the sectional surface, along the ablated surface.

Keywords: Titanium alloys, Nitinol, Surface quality

1. Introduction

In the past decades, laser-machining process became dominant and promising in most engineering and industrial fields. Laser micro-processing such as ultra-short pulse laser ablation plays an important role in the industry and research field in recent years. Application of laser micro-processing becomes more and more popular because it has the particular advantages. The laser micro-processing could be used for processing variety materials, especially on some extremely hard materials and which other conventional processing was not able or difficult to machine them.

Undoubtedly, laser ablation process is a relative new and feasible alternative to conventional processes, and the most important, shows great advantages in practical applications. First of all, this novel process does not need to contact with the workpiece. This feature allows no tool breakage or tool wear and so that it also reduces the tool cost. It can also reach those places that are really deep in cavities [1]. Besides, laser pulses parameters, such as pulse duration, frequency and position can be set precisely before machining programme. This means that high peak power can be achieved because of the high peak energy, resulting good surface performance even for microstructures. Even more, laser radiation can be converged onto a spot area, offering high-energy intensity.

Such high power and short duration on a spot allow machining hard materials which cannot be achieved by conventional processes, such as for titanium and nickel-based alloys. These alloys exhibit excellent strength, toughness, resistance to fatigue and corrosion. Hence, they have been widely used in aerospace, chemical and petrochemical, automotive and other industries. Owing to their good biological compatibility and lightweight, they are also popular in biomedical industry and medical devices especially for implants like joint replacements and bone fixations. However, their superior mechanical

doi:10.1016/j.procir.2014.04.071

properties make them very difficult to be machined by traditional processes. Moreover, these alloys can also generate high tool wear rate than other materials. In addition, their low thermal conductivity is another major challenge in machining because they will increase the temperature of tool edges and generate abrasive particles, which also increase tool wear rate and cause surface defects. Another problem is that microstructural alternations are observed as work-hardened layers due to the strain loading from conventional processes. Consequently, laser machining process is especially suitable for processing these difficult-to-machine alloys.

However, limitation and disadvantages of laser machining process are still existed and should be noticed in processing these alloys. When ablating, if the interaction time is long enough for bulk material to absorb enough energy from the laser radiation, and a thermal wave will also propagate into the bulk material, the material reach a thermodynamic equilibrium with the laser electrons and start to melt [2]. A ration of the molten material will be ejected while others remain on the surface. A recast layer is then formed on the surface when heat dissipates [3]. Besides, other negative effects, like micro-cracks, ripple pattern, debris and heat-affected zone are all easily to be caused, which resulting in a negative impact on surface quality. Therefore, the evaluation of surface finishing after machining is significant and necessary in order to predict the processing achievement and to precisely produce the desired component.

Surface quality of the machined component is one of the most important considerations when referring to certain material or evaluating design and manufacture processes. In general, it measures the metallurgical condition of machined surface and indicates the actual structure of surface and subsurface of the bulk material. The assessment of surface integrity generally includes surface roughness, residual stresses, micro-hardness, white layer formation, microstructure transformation and so on. Recently, evidences have shown that different surface integrity by varying machining parameters lead a wide range of functional performance of machined products [4]. Nevertheless, studies on surface integrity induced by laser processes are still limited, especially on NiTi and Ti6Al4V using picosecond laser.

2. Experimental setup

In this study, ablations of alloys were achieved by a High-Q picosecond laser system (High-Q IC-355-800ps, Photonics Solutions) with beam focused by a scanning galvanometer system (Nutfield-XLR8) with focus length f=100mm and idealized beam waist $2\omega_0$ ~20μm. Single craters, linear tracks and pockets (2mm×2mm) were processed on the surfaces of two alloys, Ti-6Al-4V and NiTi, using a 10-picosecond pulse laser at Infrared wavelength (1064nm) and repetition rate of 5kHz. The selected output pulse energy was from 2μJ to 16μJ with a maximum pulse number of 100 per spot, and the scanning speed was set from 5mm/s to 300mm/s. Pockets were crossed-sectioned using a 'Struers Accutom' precision wafering machine, Sectioned samples were then hot mounted in 'Metprep Conductomount' thermosetting resin, polished and etched. All the specimens were examined by a Scanning Electronic Microscope (JEOL JSM-6610).

3. Results and Discussion

3.1. Ablation threshold fluence

The ablation threshold fluence F_{th} is defined and used to illustrate the minimum fluence required for a work-piece surface to be ablated by a laser beam. For a Gaussian beam, it has been proved that the ablation threshold fluence can be obtained from Equation (1),

$$D^2 = 2\omega_0^{\,2} \ln\left(F_0 / F_{th}\right) \quad (1)$$

where D is the ablated craters diameters, ω_0 is the beam waist radius, F_0 is applied peak fluence, and F_{th} is the surface damage fluence.

A linear equation can be drawn by plotting D^2 and the logarithm of laser peak fluence ln (F_0). By extrapolation of D^2 back to zero, the ablation threshold value F_{th} can be achieved.

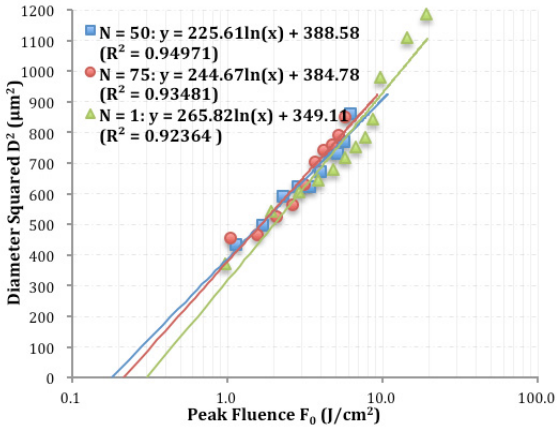

Fig. 1 Plot of D^2 versus ln(F_0) for single craters in Ti-6Al-4V ablated under laser energy between 2μJ and 40μJ with different incident pulse numbers (N = 1, 50, 75 times).

Figure 1 as an example shows the plot of D^2 versus $\ln(F_0)$ for Ti-6Al-4V plate along with solid lines fit for different pulse numbers N. The values of F_{th} for single craters on Ti-6Al-4V are then inferred to be 0.27J/cm^2, 0.18J/cm^2 and 0.21J/cm^2 for single pulse, 50 pulses and 75 pulses, respectively. The values of calculated F_{th} for Ti-6Al-4V and NiTi with different pulse numbers were compared. It is noted that generally, the value of F_{th} for single pulse craters is higher than those of multiple-pulse craters (e.g. NiTi F_{th} =0.26, 0.21, 0.15 J/cm^2 for N=1, 25 and 50, respectively). Some works [1]–[3] have been done in femtosecond laser to prove such phenomenon called incubation effect, which will be discussed following.

3.2 Incubation effect

Incubation effect is usually existed in the multiple pulse ablations and is caused by the accumulation of heat and plastic deformation. Owing to this effect, the threshold values will significantly decrease when more numbers of pulses shooting on the same spot. As above-mentioned discussion, slight reduction of threshold fluences with increasing pulse numbers can be found both for Ti-6Al-4V and NiTi alloys. The incubation effect of multiple-pulse laser ablation in picosecond laser micromachining can be explained by an incubation model [5-7],

$$F_{th}(N)=F_{th}(1)\cdot N^{S-1} \quad (2)$$

where N is the number of pulses, S is incubation coefficient.

The incubation coefficient S is a measure of the degree of incubation occurred in a material, and it can be obtained by logarithmic plotting the accumulation fluence $N^* F_{th}(N)$ and N. With the thresholds results for two alloys, Figure 2 shows the accumulation curves for Ti-6Al-4V and NiTi of multiple-pulse laser ablation. From these two curves, the incubation coefficients S are evaluated to be 0.92 for Ti-6Al-4V and 0.90 for NiTi. These two values of S are relatively high compared with other materials reported in the literature [6-7], such as Stainless Steel with 0.86, Copper with 0.87, Niobium with 0.88, pure Titanium with 0.83 and polymers with 0.7. The higher value of S indicates a weaker accumulation behavior would occur with multiple-pulse laser ablation, resulting in a smaller damaged area (i.e. less heat accumulated and plastic deformed) on the surface of workpieces with the same laser fluence. Hence, higher S could be an advantage in micro-machining processes, because the geometry accuracy of the component can be maintained when increasing the material removal rate. From this aspect of view, Ti-6Al-4V and NiTi compare favorably with other materials mentioned above. The S value for Ti-6Al-4V is found to be slightly larger than that for NiTi; this can be plained by its shorter electron-phonon coupling time of Ti-6Al-4V.

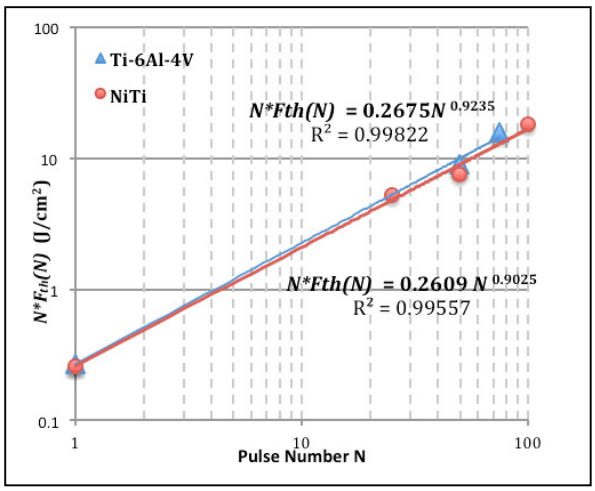

Fig. 2 Multiple-pulse incubation behavior curves for Ti-6Al-4V and NiTi alloys.

3.3 Morphological analysis

Besides quantitative analysis discussed above, qualitative observation is another essential issue when referring to the machining quality of laser materials processing. Morphological analysis of the ablated area after irradiating is especially significant because it shows the evaluation of morphological changes of the workpiece under irradiating and it can indicate the different mechanisms of material removal as the incident energy changes.

In this study, laser-ablated single craters were investigated to study the evolution of ablating processes and mechanisms of material removal under different parameters. A series SEM images of single craters ablated on Ti-6Al-4V plate with 50 times pulses per crater and increasing peak fluences are shown in Figure 3. Throughout the process of increasing energy densities, the ripple patterns are observed with periodicity of approximately 1000nm (close to the wavelength of 1064nm). Such phenomenon is well known in laser irradiation and has been named Laser-Induced Periodic Surface Structures (LIPSS) [8]. The periodic structures are always oriented perpendicular to the polarisation direction of the laser beam [6]. At lower fluences from 1.05 J/cm^2 (Figure 3 (a)), the clear ripple patterns are obtained. Between ripples, some micropores align along lines perpendicular to the ripples can also be observed. During these fluence range where ripple patterns growth, little evidence of material melting can be observed under SEM, indicating

a mechanism of equilibrium vaporisation for the material removal. This morphology result shows good machining quality and high accuracy. As the fluences increased to 2.63 J/cm^2 (Figure 3 (b)), the ripples are still clear in the outer region of the damaged area. But in the center region, some 'bridges' between the ripples are observed indicating the start of melting in the central area. When fluence is increased to 3.68 J/cm^2 (Figure 3 (c)), the ripples start to join with each other so the micropores start to disappear in the central area, where some liquid flow has occurred. As the fluence increased further, obviously melting and re-solidified area is observed. Phase explosion [9] can be used to explain this phenomenon. It can be estimated that the molten liquid has reached its critical point temperature and then massive nucleation occurred. This applied high energy density is strong enough to collapse the crystal structures, turning the material into a mixture of vapor and liquid droplets. Such morphology finishing is result from a quick expulsion of these two-phase droplets followed by a rapid cooling and re-solidified process [10].

To further understand the effects of process parameters on the surface quality of ablated samples, overlapped craters (i.e. linear tracks) were investigated by varying the overlapping rate and laser energy. This progress aims to optimize the process parameters for better surface achievements and is very essential for the following study of pocket machining. Figure 4 are the corresponding SEM results, in which Figure 4(a)-(c) are at constant scanning speed whileas Figure 4(d)-(f) are at the constant energy output. At a constant scanning speed (Figure 4(a)-(c)), the widths of the linear tracks are increased when increasing the laser energy output. The top surface and linear track are relatively smooth without any evidence of material melting at very low energy (Figure 4 (a)). At relative higher energy range (Figure 4 (c)), obvious melting and re-solidified phenomenon can be observed in the ablation area. Processed with the same energy output, it can be seen from Figure 4(d)-(f) that the track widths increase as the scanning speed decreases. Relative 'straight' lines can be obtained with the scanning speed no higher than 20mm/s. This is because the accumulation of heat and deformation in the outer region of the beam is more obvious at a lower scanning speed. Therefore, for ablating linear tracks on Ti-6Al-4V plate, relatively slow scanning speed is suggested at low energy output if the accurate dimensions are required. A prediction is achieved that when increasing the applied energy density, the scanning speed can be also increased a little bit while still control the desired geometrical accuracy.

In order to study the surface achievement of picosecond laser ablation, both the top surface and cross-sectioned surface of the machined pockets on two alloys will be investigated. Geometrical accuracy was first investigated as shown in Figure 5. It can be seen that the left and right edges of the pockets are very 'bright'. This is because more pulses have worked on these two edges due to the changes of beam directions. Measurement results show that the pocket lengths are 2.1315±0.0975mm for Ti-6Al-4V and 2.146±0.024mm for NiTi under this experimental condition. The corners of ablated pockets on two alloys are arc-shaped with a certain curvature instead of sharp right, with diameters becoming decreased when increasing the overlapping rate or decreasing the applied energy. In addition, the circles on NiTi plate are larger than those on Ti-6Al-4V, indicating a stronger ablation rate occurred on NiTi under the same process parameters.

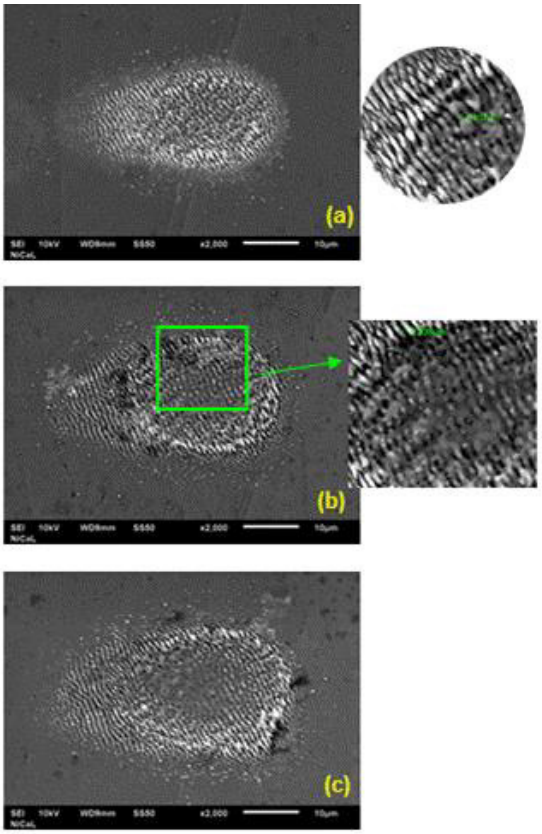

Fig. 3 SEM results for laser ablated single craters on Ti-6Al-4V with pulse numbers N = 50 times. The peak fluences F_0 are (a) 1.05 J/cm^2, (b) 2.63 J/cm^2, (c) 3.68 J/cm^2.

With the observation of cross-sectional surfaces under SEM, some 'cavities' can be found along the ablated surfaces. Figure 5 (a) shows the cavity-like feature in the pockets on Ti-6Al-4V plate. On the right side of the cavity, the surface is very flat. While on the left side and

inside the cavity, the surface is jagged. Figure 5 (b) is a magnified image of the jagged surface. The measured jag distance 0.921μm is very close to the ripple distance. Hence, it can be surmised that the jagged structure is LIPSS and the cavity is the transectional view of the right edge of the observed pocket. Then the flat surface is estimated to be parent materials without ablation. This surmise is further confirmed by measuring the width of the cavity. Its measured value 24.5μm (Figure 5(a)) is very similar to that value of edge width, 25.5μm The measured depth for this cavity is 7.0μm. A similar cavity with 23.5μm wide and 4.83μm deep was found on the NiTi pocket ablated with the same parameters. Little evidence of microstructral alternation or heat-affected zone can be found in this whole experiment. One possible reason for this is the applied energy is too small [11] or the scanning speed is too fast to cause any obvious thermal effects on the irradiated surface. Birnbaum et al. [12] has shown the microstructures of NiTi alloy can be transformed with laser power of 250w, scanning speed of 15mm/s and spot size of 7mm. The observation of sectioned surfaces in this experiment indicates the component is less likely to suffer microstructural transitions or other thermal effects when ablated with similar process parameters in the machining process.

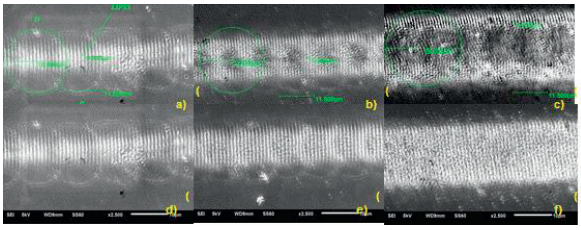

Fig. 4 Laser-ablated linear tracks on 2mm thick Ti-6Al-4V. For (a)-(c), the scanning speed is 50mm/s.; the output energy values are 2μJ, 4μJ and 10μJ, respectively. For (d)-(f), the energy output is 2μJ; the scanning speed is 50mm/s, 40mm/s and 20mm/, respectively

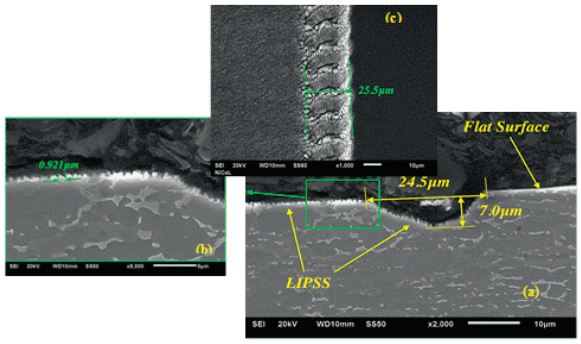

Fig. 5 SEM image of cross-sectional surface (a) of the pockets generated on Ti-6Al-4V plate with energy output of 8μJ and overlapping rate of 70%. (b) shows the details of LIPSS. (c) shows the edge width from the view of top surface

4. Conclusion

The mechanisms of material removals under different influence regimes and evolution of surface modification in the laser ablation process have been studied in this experiment. Threshold fluences, incubation effect and surface morphology of the single craters were investigated. The threshold fluences tend to be decreased when increase the pulse numbers. Ti-6Al-4V has higher incubation coefficient than NiTi, indicating its week accumulation ability of heat of plastic deformation. After inspecting on the surface morphology, a progress of ripples growth, melting and re-solidifying, phase explosion was observed as the fluence increases in the ablation process.

The influences of applied laser energy and scanning speed (overlapping rate) on machined surface were investigated on the linear tracks (overlapped craters). It can be found that higher energy generates wider tracks and more material removals while worse surface finish. Lower scanning speed ensures better dimensional accuracy for the track edges. At the same energy output and scanning speed, NiTi gives wider tracks than Ti-6Al-4V. The surface quality of the laser-ablated pockets was evaluated through an analysis on geometry accuracy, surface morphology, pocket edges and corners and cross-sectioned surfaces. The pocket lengths and widths are appeared to be slightly larger than the theoretical values. Cavity-like structures are observed along the ablated surface when inspecting the sectional surface.

5. Acknowledgements

The authors would like to acknowledge the experiments carried out at Nano Investigation Centre of Liverpool (NiCal) for providing access to Scanning Electronic Microscope and the Laser Engineering at the University of Liverpool.

References

[1] Petkov, P.V., Dimov, S.S., Minev, R.M. & Pham, D.T. 2008, "Laser milling: Pulse duration effects on surface integrity", Proceedings of the Institution of Mechanical Engineers, Part B: Journal of Engineering Manufacture, vol. 222, no. 1, pp. 35-45.

[2] Brousseau, E.B., Dimov, S.S. & Pham, D.T. 2010, "Some recent advances in multi-material micro- and nano-

manufacturing", International Journal of Advanced Manufacturing Technology, vol. 47, no. 1-4, pp. 161-180.
[3] Teixidor, D., Ferrer, I., Ciurana, J. & Özel, T. 2013, "Optimization of process parameters for pulsed laser milling of micro-channels on AISI H13 tool steel", Robotics and Computer-Integrated Manufacturing, vol. 29, no. 1, pp. 209-218.
[4] Daymi, A., Boujelbene, M., Ben Amara, A., Bayraktar, E. & Katundi, D. 2011, "Surface integrity in high speed end milling of titanium alloy Ti-6Al-4V", Materials Science and Technology, vol. 27, no. 1, pp. 387-394.
[5] N. Uppal and P. S. Shiakolas, “Micromachining Characteristics of NiTi Based Shape Memory Alloy Using Femtosecond Laser,” J. Manuf. Sci. Eng., vol. 130, no. 3, p. 031117, 2008.
[6] P. Mannion, J. Magee, E. Coyne, G. O’Connor, and T. . Glynn, “The effect of damage accumulation behaviour on ablation thresholds and damage morphology in ultrafast laser micro-machining of common metals in air,” Appl. Surf. Sci., vol. 233, no. 1–4, pp. 275–287, Jun. 2004.
[7] S. Baudach, J. Bonse, J. Krüger, and W. Kautek, “Ultrashort pulse laser ablation of polycarbonate and polymethylmethacrylate,” Appl. Surf. Sci., pp. 3–8, 2000.
[8] N. G. Semaltianos, W. Perrie, J. Cheng, P. French, M. Sharp, G. Dearden, and K. G. Watkins, “Picosecond laser ablation of nickel-based superalloy C263,” Appl. Phys. A, vol. 98, no. 2, pp. 345–355, Sep. 2009.
[9] J. Cheng, C. Liu, S. Shang, D. Liu, W. Perrie, G. Dearden, and K. Watkins, “A review of ultrafast laser materials micromachining,” Opt. Laser Technol., vol. 46, pp. 88–102, Mar. 2013.
[10] J. Huang, Y. Zhang, and J. K. Chen, “Ultrafast solid–liquid–vapor phase change of a gold film induced by pico- to femtosecond lasers,” Appl. Phys. A, vol. 95, no. 3, pp. 643–653, Mar. 2009.
[11] A. Luft, U. Franz, a. Emsermann, and J. Kaspar, “A study of thermal and mechanical effects on materials induced by pulsed laser drilling,” Appl. Phys. A Mater. Sci. Process., vol. 63, no. 2, pp. 93–101, Jul. 1996.
[12] A. J. Birnbaum and Y. L. Yao, “The Effects of Laser Forming on NiTi Superelastic Shape Memory Alloys,” J. Manuf. Sci. Eng., vol. 132, no. 4, p. 041002, 2010.